Growth and morphology of Cobalt thin films on Pd(1 1 1)

M. Wasniowska [a,b,*], N. Janke-Gilman [a], W. Wulfhekel [a,c], M. Przybylski [a,b], J. Kirschner [a]

[a] *Max-Planck-Institut für Mikrostrukturphysik, Weinberg 2, 06120 Halle, Germany*
[b] *Solid State Physics Department, Faculty of Physics and Applied Computer Science, AGH University of Science and Technology, Mickiewicza 30, 30-059 Kraków, Poland*
[c] *Physikalisches Institut, Universität Karlsruhe, Wolfgang-Gaede Strasse 1, 76131 Karlsruhe, Germany*

Abstract

We report on the growth of thin Co films on Pd(1 1 1) at three different temperatures 180 K, 300 K, and 550 K. The structure and morphology was determined by scanning tunneling microscopy and low energy electron diffraction. The growth mode was found to vary with temperature. For 180 K and 300 K, we observed a tendency to double layer growth for the initial layers while at elevated temperatures, the initial film grows in single layer. For most conditions, non-ideal three-dimensional growth was observed. Two-dimensional growth was only found for growth temperature of 550 K and coverages above 5 ML. Depending on temperature, the Co islands at low coverages exhibit three principally different shapes: dendritic at 180 K, hexagonal at 300 K and triangular at 550 K. For growth at 550 K and coverages above 5 ML, the islands changed to an irregular shape. This transition is most likely responsible for the transition to 2D growth. Further, the large strain is relaxed by the creation of a dislocation network with mixed fcc and hcp stacking. Depending on the temperature and coverage, a hexagonal or a triangular network was observed. Finally, we have investigated the effect of annealing Co films prepared at 180 K and 300 K. Heating to 490 K leads to coarsening and intermixing.
© 2007 Elsevier B.V. All rights reserved.

Keywords: Growth; Cobalt; Palladium; Single crystal epitaxy; Low energy electron diffraction; Scanning tunnelling microscopy

1. Introduction

In recent years, the properties of Co on Pd(1 0 0), Pd(1 1 0) and Pd(1 1 1) surfaces as well as Co/Pd multilayers have been a matter of detailed investigations [1–4]. These systems are of current scientific and technological interest. Co/Pd systems are candidates for magneto-optic recording media because they have a high perpendicular magnetic anisotropy in thin films, high coercivities and large magneto-optic Kerr (MOKE) signals [2,5]. Beside these properties, Co/Pd similar to Fe/Pd systems show additional attraction due to their exotic exchange coupling leading to an induced magnetization of Pd at the interface (hybrid-ization of Pd 4d and Co 3d states) [6,7]. Since magnetic properties are very sensitive to the details of Co/Pd interface, a thorough knowledge of the growth process in this system is essential. Highly important process parameters influencing the film morphology are the substrate temperature and surface free energies of the substrate and the film. The surface free energy of Pd(1 1 1) is $\gamma_{Pd} = 1.61$ J/m^2 which is lower than that of Co $\gamma_{Co} = 2.0$ J/m^2 [8]. In the thermodynamic limit, this leads to three-dimensional growth of Co islands. Further, the lattice mismatch between Co and Pd is large (9.1% compressive strain) opposing smooth Co films. The question of pseudomorphic growth of the first few Co layers is, however, still discussed controversially. In recent years, the system Co on Pd(1 1 1) has been studied intensely and a large number of experiments with various techniques have been reported. The growth of Co films on Pd(1 1 1) in the different coverage regimes is nevertheless not well understood. In the literature,

---

* Corresponding author. Address: Max-Planck-Institut für Mikrostrukturphysik, Weinberg 2, 06120 Halle, Germany. Tel.: +49 345 5582667; fax: +49 345 5511223.
E-mail address: mwasnio@mpi-halle.de (M. Wasniowska).

Co on Pd(1 1 1) was deposited mostly at room temperature. Only in one work, deposition at elevated temperature (370 K) [10], was reported. Several morphological studies revealed that Co in the low coverage region does not show a two-dimensional growth (layer-by-layer). Atrei et al. [11] examined the system Co/Pd(1 1 1) using a combination of low energy ion scattering (LEIS) and X-ray photoelectron spectroscopy (XPS) measurements. They claim that multilayer Co islands grow with variable thickness. They proposed a Volmer–Weber growth mode. The low electron energy diffraction (LEED) patterns remained of (1×1) symmetry for all coverages, i.e., they did not observe additional spots due to relaxation. Their conclusion was that the Cobalt islands are tetragonal distorted fcc and the Co film is presumably pseudomorphic. Similar observations were reported by Oh et al. [12] by means of X-ray photoelectron diffraction (XPD). Co was found to grow in islands of fcc structure. LEED measured after the evaporation showed, however, diffuse patterns as the films thickness increases. Yokoyama et al. [13] and Purcel et al. [14,15] ruled out layer-by-layer growth mode due to lack of reflection high energy electron diffraction (RHEED) oscillations. Purcel et al. [14,15] reported that Co grows epitaxially up to 12 ML, incoherently and relatively flat on Pd(1 1 1). Moreover, LEED patterns with additional six-fold arrays of spots reminiscent of a Moiré pattern were observed. The LEED patterns are similar to those reported by Boukari et al. [10,16] clearly indicating non-pseudomorphic growth. For both 300 K and 370 K, they observed three-dimensional films, which are composed of about 50% hcp Co and 50% disorder Co for samples prepared at 370 K. Kim et al. [17,18] found evidence that Co grows epitaxially on palladium in a layer-by-layer mode, gradually turning into 3D structures (mounds) for thicker films. Their scanning tunneling microscopy (STM) images confirm a layer-by-layer growth on flat Pd crystals. The surface morphology at submonolayer coverage is characterized by small monolayer high islands.

In this paper, we report on systematic investigations on the growth mode and the structure of Co on Pd(1 1 1). To gain reliable information, we performed combined STM and LEED studies as a function of deposition temperature and coverage. We show that the growth of Co on Pd(1 1 1) reacts sensitively to changes of the growth parameters, which explains the contradictory findings of different groups.

2. Experimental set-up

Experiments were performed in an ultra-high vacuum (UHV) chamber with a background pressure better than 1.0×10^{-10} mbar. The chamber was equipped with LEED, Auger electron spectroscopy (AES), MOKE and a home-built low temperature STM. The surface of the crystal was cleaned with cycles of 1.5 kV Ar$^+$ sputtering and annealing to 870 K. AES spectra of the single crystal showed no contamination; especially the S and O peaks

were below the detection limit of our spectrometer. Sharp (1×1) LEED patterns with three-fold symmetry which are characteristic of clean fcc Pd(1 1 1) surfaces were observed after this treatment. STM images resolved clean, flat terraces of sizes larger than 150 nm separated by single atomic steps 2.20 Å high. Co (99.999% purity) was deposited using electron beam evaporation. The pressure during the growth process remained below 1.0×10^{-10} mbar. The deposition rate was about 0.4 ML/min (in Pd(1 1 1) substrate atomic density units). The Co evaporation rate was calibrated using medium energy electron diffraction (MEED) intensity oscillations during layer-by-layer growth of Co on Fe(0 0 1). The deposition of Co films on Pd(1 1 1) was performed at different substrate temperatures, i.e., at 180 K (low temperature), 300 K (room temperature) and 550 K (elevated temperature). The sample temperature was measured with a thermocouple attached to the sample holder in close vicinity of the sample and with a pyrometer. The upper temperature (550 K) was chosen as a limit above which strong interdiffusion of Co into Pd occurs. Some films were deposited at 300 K or at 180 K followed by a gentle annealing to 490 K for about 10 min. After growth, LEED and STM were carried out at 300 K or below.

3. Results

We will present the experimental results in the following way. First, we concentrate on the growth of Co on Pd(1 1 1) at 300 K. Next, we focus on growth at low temperatures (180 K) and at elevated temperatures (550 K). Finally, to complete the study on the growth, we investigated the effect of annealing of samples prepared at 300 K and 180 K.

3.1. Film growth at 300 K

The growth and morphology of Co layers in the thickness range up to 12 ML deposited at room temperature was investigated. In the submonolayer regime, Co grows as double-layer islands, as can be seen in Fig. 1a for the coverage of 0.6 ML. The line scan in the Fig. 1b shows
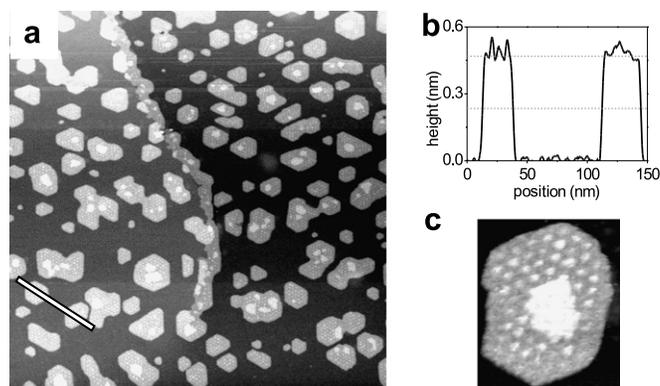
Fig. 1. (a) STM image after deposition 0.6 ML Co on Pd(1 1 1) at 300 K (500 nm × 500 nm); (b) line profile across two islands along the line shown in (a); (c) hexagonal island with dislocation pattern (43 nm × 47 nm).

an island height of 4.6 Å at a sample bias of 1 V. The average island separation is 50 nm and the islands are hexagonal reflecting the surface symmetry. Similarly shaped islands have also been observed during growth of Co/Pt(1 1 1) [19] and Co/Au(1 1 1) [20]. Not all deposited material ends up in the islands on the terraces. Similar to nucleated islands, substrate steps also act as sinks for the Co adatoms. Some of the deposited material tends to decorate the lower step edges at low coverage while at higher coverages, both the upper and lower step edges are decorated with Co. On top of the islands, STM images show a regular pattern of protrusions appearing as white dots. This superstructure, a dislocation pattern, can be seen in more detail in the zoom of Fig. 1c. The large lattice mismatch between Co and Pd of 9.1% prevents a pseudomorphic growth. Instead, the Co film relaxes via dislocation formation. This relaxation is facilitated by the fact that the fcc (1 1 1) plane is the glide plane and the formation of dislocations in Co/Pd is easy. The dislocation formation results in the regular superstructure reminiscent of a Moiré pattern. Due to the relaxation mechanism, regions with local hcp and fcc structure with respect to the substrate are formed. They are separated by atoms in a bridge position forming a structural domain wall [21]. In Co/Pd(1 1 1), the dislocation network is located most likely at the substrate adsorbate interface, but can still be detected in STM images of up to 10 ML thick films deposited at 300 K (see Fig. 2d). Note that it was impossible to determine whether thick Co films grow in fcc or on hcp stacking sequence solely based on the

lattice constant of the dislocation pattern. This is due to the only slightly different lattice distance for fcc Co(1 1 1) and hcp Co(0 0 0 1). It was, however, possible to differentiate between fcc or hcp stacking sequence by means of scanning tunneling spectroscopy (STS). STS curves for the two types of stacking are similar, but differ by a shift in energetic position of the surface state peak. Using this effect, the identification of the stacking was possible with lateral resolution as will be reported elsewhere [22]. Within the unit cell of the dislocation pattern, both fcc and hcp areas could be found in agreement with the relaxation of stress via dislocation formation and gliding. The fact that the islands are formed as double layers indicates a tendency of the Co atoms that are deposited on the Pd terraces to diffuse upward on top of the first layer of Co. Assuming local thermodynamic equilibrium at the rim of the growing islands, this implies a stronger binding of atoms in the second layer compared to the first layer. At 0.6 ML, one even observes small third-layer islands on top of the larger Co islands. Possibly third and next monolayers nucleate on the network of dislocations due to a restricted diffusion across dislocation lines [21]. Fig. 2 shows a series of STM images of Co on Pd(1 1 1) with various coverage. The first Co double-layer islands start to percolate at about 2.3 ML (see Fig. 2a). At this coverage, the third layer nucleates on most of the islands. In Fig. 2b, corresponding to a coverage of 3 ML Co, the surface of Pd is still visible, while the fifth layer starts to nucleate. Also these STM images for each coverage directly show that the island sizes
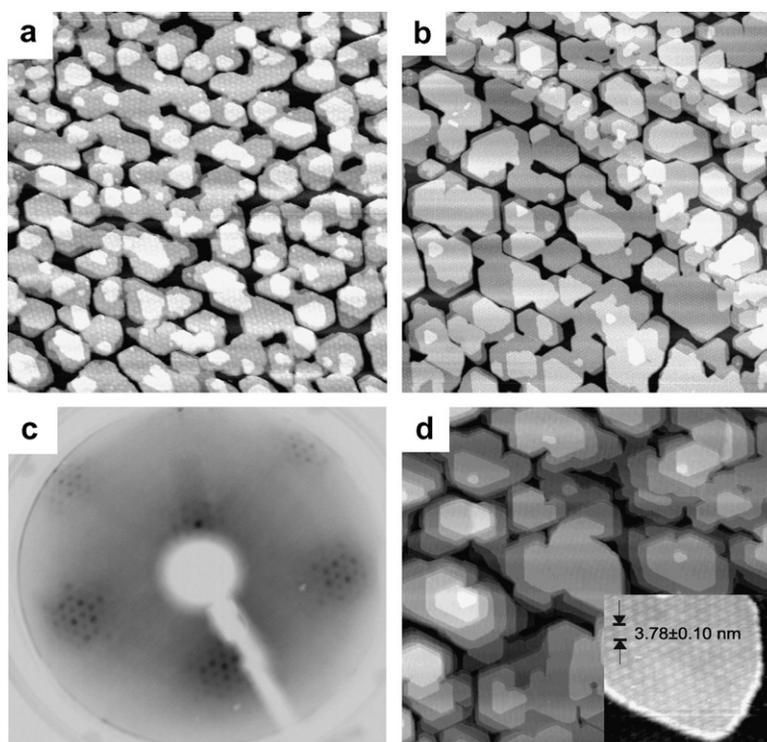
Fig. 2. STM images after deposition at 300 K of (a) 2.3 ML; (b) 3 ML; (d) 10 ML Co/Pd(1 1 1). Size is always 500 nm × 500 nm. The inset in (d) shows the dislocation pattern (55 nm × 55 nm). The black arrows indicate the distance between two corrugations. The periodicity of dislocation pattern was measured to be 3.78 ± 0.10 nm; (c) LEED diffraction pattern of 2.3 ML Co/Pd(1 1 1) taken at 190 eV.

become larger as the Co coverage is increased. At 10 ML, the film is rough with deep trenches (see Fig. 2d). At this coverage, the island shape has changed. It is mainly triangular for thick films while it is hexagonal at lower coverage, and the dislocation pattern can still be detected in STM images of up to 10 ML thick film. The observed periodicity of the pattern of 3.78 ± 0.10 nm on the 10 ML thick island agrees well with the expected periodicity of the Moiré pattern of 3.38 nm for the misfit of 9.1%. This can be understood on the basis of the low energy needed for gliding between fcc and hcp stacking in the fcc(111) plane. As a consequence, the dislocation energy is low and a distinction between a Moiré pattern and a dislocation network becomes essentially meaningless. Our topographic STM results differ from the results reported by Kim et al. [17,18] which showed that for comparable growth rate and temperature, Co grew in layer-by-layer mode for the first monolayers. Concerning the determination of the growth mode, the area fraction of the atomic levels was estimated from the STM images of Fig. 2. While the STM images qualitatively show a 3D growth mode, Fig. 3 shows the layer distribution obtained from the STM images which gives a criterion to distinguish between 2D and 3D growth. In the case of ideal 2D growth, interlayer diffusion across step edges to a lower terrace has to be present, resulting in a limited number of open levels, three levels at most. In the case of ideal 3D growth, in which no interlayer diffusion is present, the distribution of the terrace levels is expected to follow the Poisson distribution [19,23,24]. The Poisson distribution is plotted as black line. Fig. 3a and b show that the experimental data points do not agree well with ideal 3D growth. More material is found in the lower layers than is expected for ideal 3D growth. This shows that some mass transport from the higher layers to the lower layers is present. It can be seen from Fig. 3, that the layer distribution for thicker films is closer to that of ideal 3D growth. While for 3 ML, ~12% of the total mass of the film is in a layer differing from the ideal 3D growth, it is ~6% for the
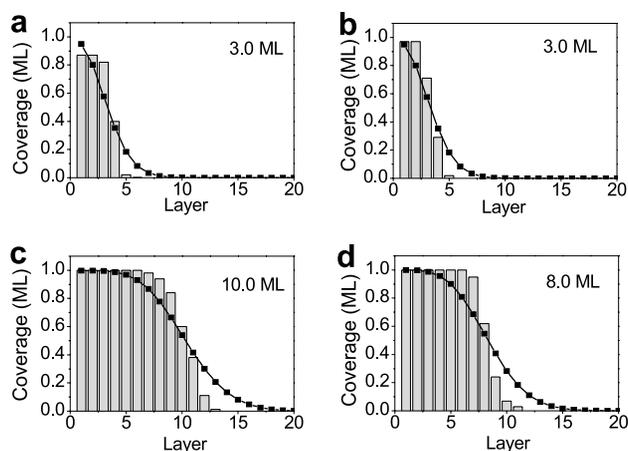
10 ML film. In summary, the STM images show that the growth is neither ideal layer-by-layer nor ideal three-dimensional. This means that interlayer transport is most likely hampered by a Schwoebel barrier, but is not completely suppressed.

A complementary probe to STM for atomic structure of films is LEED. LEED patterns of films below 0.4 ML show minor changes from the $p(1 \times 1)$ pattern of clean Pd. This situation changes with further deposition. At a coverage of 0.6 ML additional superstructure spots appear. LEED showed hexagonal patterns around all principal spots. These structures become more pronounced for higher coverage and are shown in Fig. 2c. The origin of the satellite spots in the LEED pattern is the periodic arrangement of dislocations, i.e., the Moiré structure also seen in STM. The observation of the superstructure both in STM images and LEED patterns excludes pseudomorphic growth. These results agree well with earlier LEED studies by Purcell et al. [14,15] and Kohlhepp Co/Pd(111)/W(110) [9]. The fact that the LEED pattern is of six-fold symmetry and not of three-fold symmetry as expected for fcc(111) is related to the mixing of fcc and hcp stacking within the unit cell of the dislocation pattern.

3.2. Film growth at 180 K

The morphology of Co at various coverage is illustrated in Fig. 4. The initial stage of the growth at low temperature is characterized by the formation of monolayer dendritic shape islands (cf. Fig. 4a). At low temperatures, islands nucleate at a higher density in comparison to the growth at 300 K. This is due to the reduction of the thermal mobility of the Co atoms on the Pd terraces. The average island separation of about 25 nm at 180 K, however, indicates that the atoms still have a significant mobility at this low temperature. This speaks for a low diffusion barrier in agreement with diffusion on many other fcc(111) surfaces [25]. The dendritic island shape with structural features on the length scale of only few nm is due to the fact that diffusion of adatoms that are attached to the growing islands have a mobility significantly lower than adatoms on the terraces. Thus, during island growth, the attachment of adatoms is faster than edge diffusion such that the islands do not reach a thermodynamically stable compact shape. The 0.2 ML film is characterized by 1 ML high islands with a second layer appearing as white dots on top of the islands (see Fig. 4a). The diameter of these dots is of the order of 1 nm. Next, the Co dots start to coalescence and a second layer nucleates mostly in the center of the islands.

The 2.0 ML film exhibits a morphology that is characterized by the formation of double-layer islands similar to growth at 300 K. At about 1.7–2 ML, the double layer islands start to percolate and form a network as shown in Fig. 4b. On top of the islands, a weak dislocation pattern was detected for coverages between 1.3 and 3 ML. This pattern is only faint in STM images but is much easier to

Fig. 3. Layer distribution within the film. The black line represents ideal 3D growth with no interlayer diffusion. (a) and (b) for Co/Pd(111) prepared at 300 K; (c) and (d) for samples prepared at 180 K.
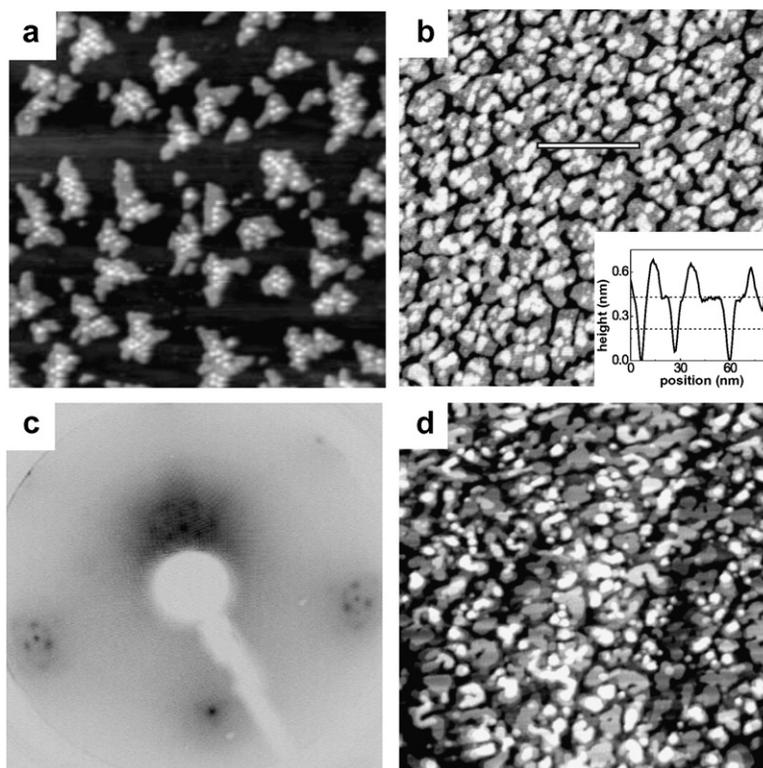
Fig. 4. STM images of Co/Pd(1 1 1) prepared at 180 K. Film coverages were: (a) 0.2 ML; (b) 2.0 ML. The line profile was taken along the line shown in the corresponding STM image; (d) 8.0 ML. The size for images is always 300×300 nm^2; (c) LEED diffraction pattern of 2 ML Co/Pd(1 1 1), $E = 140$ eV.

detect in LEED patterns for the same coverages (see Fig. 4c) due to the higher sensitivity of LEED to periodic structures. At 2 ML coverage, the third layer (shown in white) starts to nucleate before the second layer (shown in gray) is completed. This phenomenon may be taken as an evidence of the presence of a step edge barrier for diffusion across a step, i.e., a Schwoebel barrier [26], which hinders downward transport of atoms. Rough growth is characteristic also for thicker films. Films of nominal 8 ML coverage display up to five open atomic layers (see Fig. 4d). Consequently, the low temperature growth of Co on Pd is characterized by a 3D growth as shown by the layer distribution compared with the Poisson distribution in Fig. 3c and d. This indicates a suppressed interlayer mass transport of atoms that are deposited on growing islands leading to the roughening of the films. When comparing 3 ML films grown at 300 K and 180 K, the 180 K films are smoother, i.e., more material in the lower layers. Such a behaviour cannot be related to thermodynamics but is a kinetic effect. It can be due to the ramified islands shape at low temperatures which have more kinks sites than compact islands facilitating intralayer diffusion [27]. Thus, the films grown at 180 K are significantly smoother than ideal 3D growth.

3.3. Film growth at 550 K

Due to various thermally activated processes such as diffusion, migration, surface alloying, attachment or detachment from islands, the morphology is very sensitive to changes of the growth temperature. Many diffusion processes can be switched on at elevated temperatures. In this Section, we discuss the growth of Co on Pd(1 1 1) at 550 K between 0.6 and 5 ML. Fig. 5 shows wide-area STM images for the coverages of 0.6 ML, 1.7 ML, and 5 ML. At low coverage, separate islands are observed (cf. Fig. 5a). The islands are triangular, have a compact shape and are one atomic layer high in contrast to the double-layer growth at 300 K. Second layer Co islands nucleated on first-layer islands. The area of the second layer is less than 3% and no third layer could be observed. The average island separation is 70 ± 13 nm. The density of islands for samples prepared at 550 K is much lower than at 180 K and 300 K [22]. At submonolayer coverages, Co decorates the edge of the substrate steps forming 1 ML high islands. We found no hint of a reconstruction or dislocation network on the Co islands in the STM topography. Furthermore, the LEED patterns are free of a superstructure as can be seen in the Fig. 5b. This indicates that the surfaces of the islands are completely strained to the Pd lattice spacing. For 1.7 ML total coverage, the first layer is almost filled and second and third layer islands can be seen. The most striking characteristic is the observation of a corrugation on the second layer Co islands at 1.7 ML and above (see Fig. 5e) which differs from the superstructure observed in films grown at room temperature and below. The corrugation at elevated temperatures has a triangular symmetry. The superstructure was also observed with LEED, which
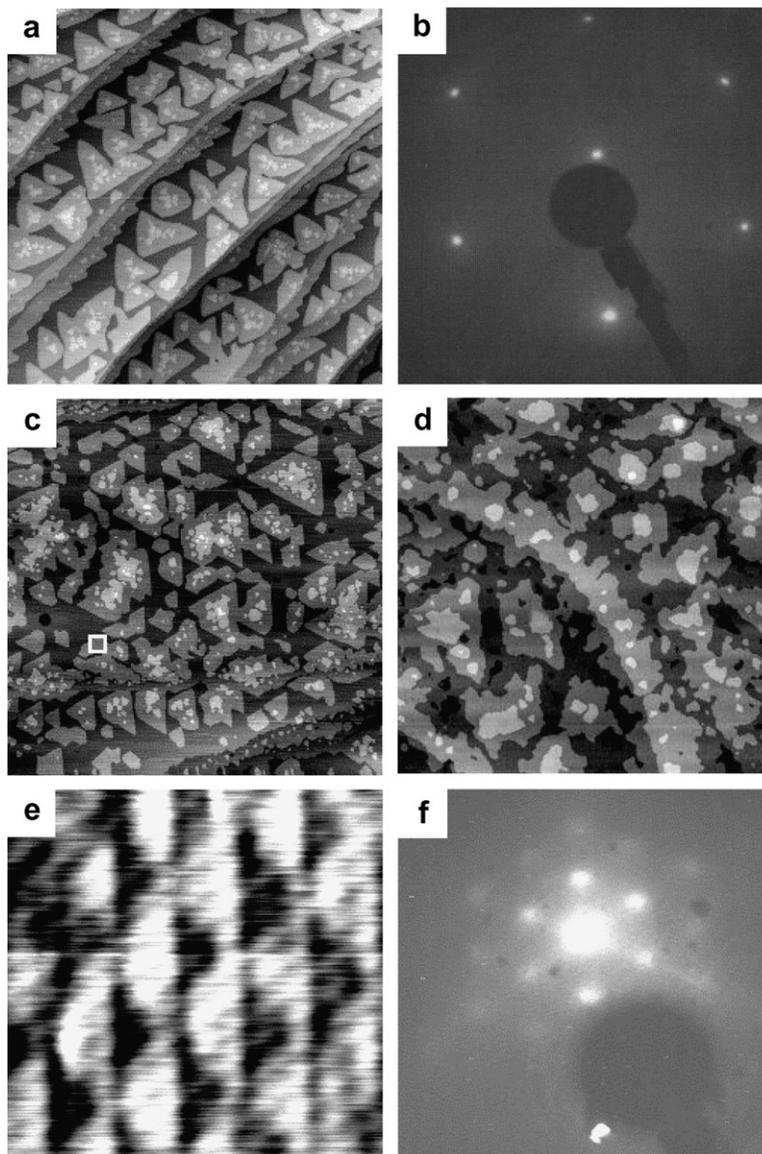
Fig. 5. STM images of Co/Pd(111) after growth at 550 K of: (a) 0.6 ML (1800×1800 nm^2); (b) corresponding LEED pattern at $E = 220$ eV for (a); (c) 1.7 ML (750×750 nm^2). The area marked in (c) is magnified in part (e); (d) 5 ML (660×660 nm^2); (e) STM topography revealing the triangular network (21 nm $\times$ 21 nm); (f) corresponding LEED pattern presenting ($0\,0$) spot for triangular network, $E = 50$ eV.

shows a hexagonal pattern around the Pd substrate spots (cf. Fig. 5f). The average distance between the center of neighboring triangles is 3.81 ± 0.46 nm. The corrugation of the triangular structure is only 0.05 nm, indicating that it is not caused by vacancies in the Co layer. Similar to the dislocation pattern observed at 180 K and 300 K, the superstructure is due to the large lattice mismatch. Most likely, the triangular boundary separates fcc and hcp regions and is a partial dislocation. Similar structural features were previously reported for Co on Re(0001) [28]. Two kinds of triangles are separated by domain boundaries, that come about by a different stacking sequence of the Co atoms in adjacent triangles (see Ref. [28]). For films grown at 550 K, a dislocation pattern similar to that of films deposited at 300 K and 180 K was observed starting from the fifth monolayer. The nearly 3D growth proceeds

up to 5 ML total coverage. The quantitative layer coverage is shown in Fig. 6. The analysis shows that the first layer is 90% complete before the third layer starts to grow. Similarly, the second layer and the third layer are not filled before the next layer appears. Such a growth mode can be caused by a scenario in which for the first layers deposited, the Co atoms cannot move freely across steps and a Schwoebel barrier is present such that islands nucleate on top of islands before the layer is completed. This barrier seems to become lower as a function of coverage and changes the growth at coverage higher than 5 ML. Fig. 6 shows that at 10.5 ML coverage, the film is much flatter and shows three open layers only. As a consequence, the layer distribution has a sharp edge. Ultra-thin Co films deposited on Pd at 550 K show a more complex growth process than the films deposited at low temperature and at room temper-
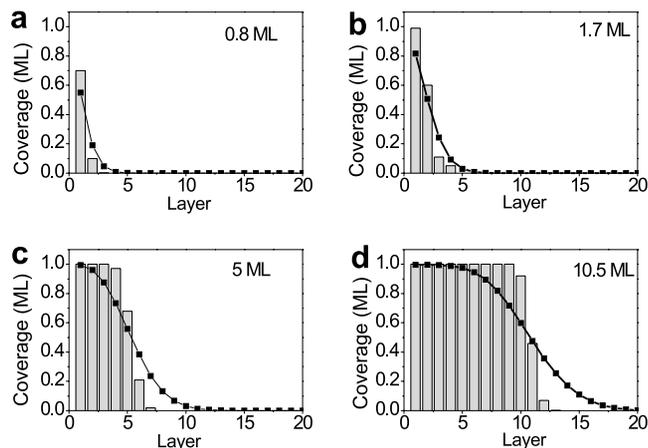
Fig. 6. Layer distribution and ideal 3D growth (black lines) of (a) 0.8 ML, (b) 1.7 ML, (c) 5 ML and (d) 10.5 ML films prepared at 550 K.

ature. The films thicker than 5 ML are almost perfectly flat and are much smoother than films deposited at 300 K or 180 K. The flatter growth above 5 ML goes hand in hand with a change of the island shape from triangular to irregular. The latter also explains the better growth as kinks in the island edge may lower the Schwoebel barrier. Such a relation was found before for Pt/Pt(1 1 1), however, at low temperatures [27]. Possibly, the appearance of the dislocation structure is linked to the changes of the growth mode. It might be the case that the structural change of the surface modifies the diffusion, i.e., the islands shape and the Schwoebel barrier.

3.4. Annealing of samples prepared at 300 K and 180 K

To complete the study of the growth of Co/Pd(1 1 1), we investigated the annealing of structures obtained by growth at low temperature and at room temperature. We measured LEED and STM for samples before and after annealing. For a detailed study of the processes occurring at elevated temperatures, we choose two samples: 1.7 ML Co/Pd(1 1 1) prepared at 180 K and 2.3 ML Co/Pd(1 1 1) prepared at 300 K. The topography of the samples before annealing showed a 3D mode of growth. After annealing, the morphology changed. First, 1.7 ML of Co was deposited at 180 K. At this low coverage, the double layer islands start to coalesce. Fig. 7a shows an STM image immediately after deposition. Following the deposition, the film was heated at a constant rate of 10 K/min. In Fig. 7b and c, the sample surface is displayed after annealing to 380 K and 490 K, respectively. In Fig. 7b, the Co islands are similar to those before annealing. The diameters of the Co islands are, however, slightly larger in comparison to non-annealed samples grown at 180 K. The layers start to spread out as indicated by the appearance of 1 ML thick areas in the line profile. Some islands began to coalesce, i.e., we see the onset of thermally activated coarsening. We further observe small depressions of subatomic height inside the islands indicating some inhomogeneity in the layers. For even higher annealing temperatures the island size further increases. After annealing up to 490 K, some islands have an elongated form, probably as the result of coalescence of smaller islands. The islands in the topmost layers are increased in
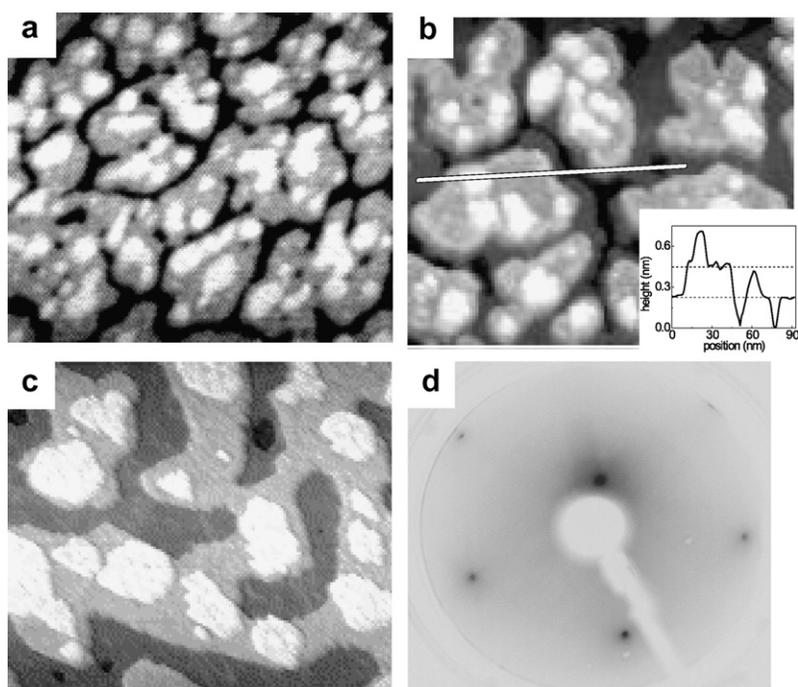
Fig. 7. STM images illustrating the thermal evolution of 1.7 ML Co on Pd(1 1 1) deposited at 180 K (150 nm × 110 nm). (a) As grown; (b) annealed to 380 K. The inset shows a line profile along the line; (c) and 490 K; (d) LEED pattern for sample annealed to 490 K (*E* = 140 eV).

size. The width of the coalesced islands is around 40 nm and the height is 1 ML. The LEED pattern for the film grown at 180 K showed the previously discussed satellite spots due to the dislocation network (see Fig. 4c). The LEED pattern for 1.7 ML film after annealing to 490 K is displayed in Fig. 7d. It shows sharp p(1 × 1) spots and the disappearance of the superstructure spots. The LEED pattern shows a higher background and the satellites surrounding the (0 0) spot have been transformed to a fuzzy halo around the principal spot. As Co and Pd have different LEED scattering factors, the blurred (1 × 1) LEED pattern may be caused by a disordered alloy of Co and Pd. At 300 K and 180 K, Co–Pd exchange process and alloying, or interdiffusion phenomena play a minor role [29]. However, higher temperatures may activate these processes. This interpretation is in agreement with the inhomogeneities observed in the STM scans after annealing to 380 K. They are most likely indications for first interdiffusion starting at 380 K that influence the LEED pattern at 490 K.

The STM measurements after deposition of 2.3 ML Co at 300 K show 3D growth. The STM images taken of the annealed film reveal morphological changes compared to the 300 K situation. Annealing to 490 K leads to completion of the first monolayer and island coarsening (see Fig. 8c). Hexagonal islands with dislocations are still visible after annealing. The annealing allows the atoms to overcome the kinetic limitations imposed by deposition at 300 K and to migrate to the Pd surface. The same effect is clearly observed for annealed Co films prepared at

180 K. The annealing of 2.3 ML Co/Pd(1 1 1) at 490 K causes a slight change of the LEED pattern. Fig. 8b and d show a typical LEED pattern before and after annealing, respectively. The annealing results in a modification of the hexagonal satellites in the pattern. The (0 0) spot is still surrounded by satellite spots corresponding to the stable dislocation pattern of the islands observed in STM. The background intensity, however, increased significantly. Additionally, the satellite peaks around the higher-order spots are much weaker after annealing. Both observations indicate an increased disorder most likely caused by formation of an unordered alloy.

4. Summary and conclusions

We have performed a systematic study of the influence of temperature on the growth of cobalt on Pd(1 1 1). The growth is strongly temperature-dependent. Three different island shapes have been found at low coverages. At 180 K, fairly irregular islands were observed due to a low mobility along step edges. At 300 K, hexagonal islands indicate an effective diffusion along step edges. The third type of islands found at elevated temperatures is characterized by smoother edges and an overall triangular shape. A three-dimensional growth mode was found and was related to a Schwoebel barrier which prevents higher layer atoms from surmounting the edges of individual islands. This way, next layer islands nucleate early in the growth process. At high growth temperatures and thickness above 5 ML,
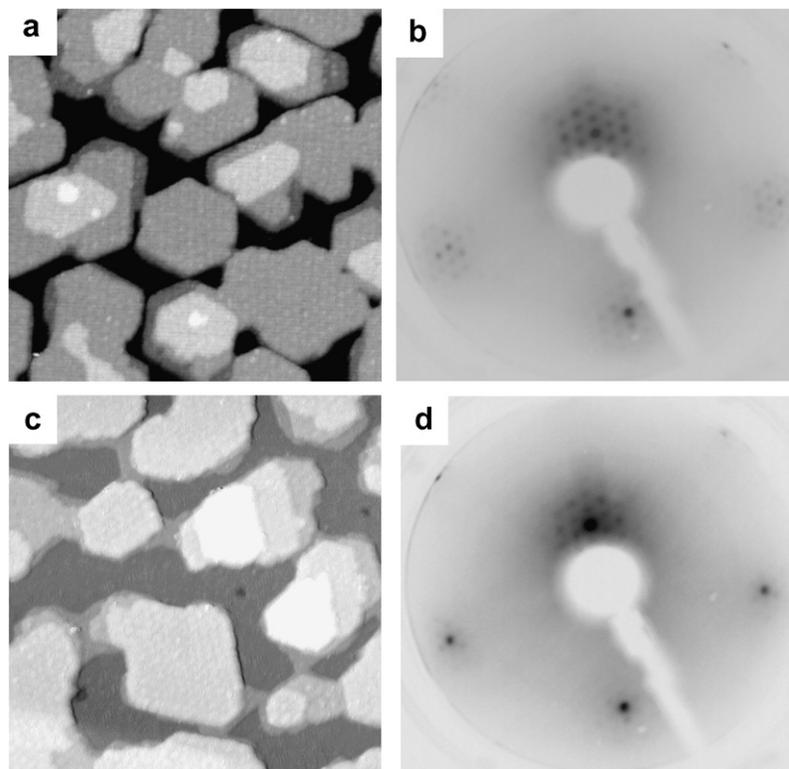
Fig. 8. STM images and LEED patterns illustrating the thermal evolution of 2.3 ML Co on Pd(1 1 1) deposited at 300 K (a), (b) before and (c), (d) after annealing to 490 K. (a), (c) size is 150 nm × 150 nm. (b), (d) at $E = 140$ eV.

the islands' shape changes to a more irregular structure with a high density of kinks. Hand in hand with this transition, the growth changes to 2D. This effect was related to a reduction of the Schwoebel barrier due to the high kink concentration. For coverages below 2 ML, double layer island growth was observed at 300 K and less pronounced at 180 K. This growth mode is most likely related to a higher binding energy of Co adatoms on the first Co monolayer than on the Pd substrate, i.e., it reflects a heteroepitaxial effect.

A hexagonal dislocation pattern was found for all growth temperatures starting with the second layer for 180 K and 300 K as well as for 5 ML at 550 K. The dislocation pattern is due to a relaxation of the heteroepitaxial lattice mismatch by dislocation formation. This implies a mixed fcc and hcp stacking in the dislocated films. At the highest growth temperature, a second and triangular superstructure was found below 5 ML. Finally, the annealing of films was studied. With increasing annealing temperature, the films were smoother but indications of intermixing were observed in STM and LEED.

References

[1] B.N. Engel, M.H. Wiedmann, R.A. Van Leeuwen, C.M. Falco, L. Wu, N. Nakayama, T. Shinjo, Appl. Surf. Sci. 60 (1992) 776.
[2] M. Przybylski, L. Yan, J. Żukrowski, M. Nyvlt, Y. Shi, A. Winkelmann, M. Wasniowska, J. Barthel, J. Kirschner, Phys. Rev. B 73 (2006) 085413.
[3] Y. Fujii, T. Komine, T. Kai, K. Shiiki, J. Phys.: Condens. Matter 11 (1999) 9601.
[4] S.-K. Kim, Y.-M. Koo, V.A. Chernov, J.B. Kortright, S.-C. Shin, Phys. Rev. B 62 (2000) 3025.
[5] S. Uba, L. Uba, A.N. Yaresko, A. Ya Perlov, V.N. Antonov, R. Gontarz, J. Phys.: Condens. Matter 10 (1998) 3769.
[6] J. Dorantes-Dávila, H. Dreyssé, G.M. Pastor, Phys. Rev. Lett. 91 (2003) 197206.
[7] F. López-Urías, J. Dorantes-Dávila, H. Dreysse, J. Magn. Magn. Mat. 165 (1997) 262.
[8] I.V. Markov, Crystal growth for beginners: Fundamentals of nucleation, crystal growth and epitaxy, World Scientific, Singapore, 1995.
[9] J. Kohlhepp, Torsion-Oszillations-Magnetometrie an ultradünnen Kobalt-Epitaxie-Schichten, Ph.D. thesis Technischen Universität Clausthal, 1994.
[10] S. Boukari, E. Beaurepaire, H. Bulou, B. Carrière, J.P. Deville, F. Scheurer, R. Baudoing-Savois, M. De Santis, Surf. Sci. 430 (1999) 37.
[11] A. Atrei, G. Rovida, M. Torrini, U. Bardi, M. Gleeson, C.J. Barnes, Surf. Sci. 372 (1996) 91.
[12] S.-J. Oh, W. Kim, W. Kim, B.-H. Choi, J.-Y. Kim, H. Koh, H.-J. Kim, J.-H. Park, Appl. Surf. Sci. 169–170 (2001) 127.
[13] T. Yokoyama, D. Matsumura, K. Amemiya, S. Kitagawa, N. Suzuki, T. Ohta, J. Phys.: Condens. Matter 15 (2003) S537.
[14] S.T. Purcell, H.W. van Kesteren, E.C. Cosman, W. Hoving, J. Magn. Magn. Mater. 93 (1991) 25.
[15] S.T. Purcell, M.T. Johnson, N.W.E. McGee, J.J. de Vries, W.B. Zeper, W. Hoving, J. Appl. Phys. 73 (1992) 1360.
[16] S. Boukari, E. Beaurepaire, H. Bulou, B. Carrière, J.P. Deville, F. Scheurer, M. De Santis, R. Baudoing-Savois, Phys. Rev. B 64 (2001) 144431.
[17] J. Kim, J.-W. Lee, J.-R. Jeong, S.-K. Kim, S.-C. Shin, Appl. Phys. Lett. 79 (2001) 93.
[18] J. Kim, J.-W. Lee, J.-R. Jeong, S.-K. Kim, S.-C. Shin, J. Appl. Phys. 89 (2001) 7147.
[19] P. Varga, E. Lundgren, J. Redinger, M. Schmid, Phys. Stat. Sol. (a) 187 (2001) 97.
[20] O. Fruchart, M. Klaua, J. Barthel, J. Kirschner, Phys. Rev. Lett. 83 (1999) 2769.
[21] K. Bromann, M. Giovannini, H. Brune, K. Kern, Eur. Phys. J.D 9 (1999) 25.
[22] M. Wasniowska, W. Wulfhekel, M. Przybylski, J. Kirschner, to be published.
[23] K. Meinel, M. Klaua, H. Bethge, J. Cryst. Growth 89 (1989) 447.
[24] K. Nobuhara, H. Kasai, H. Nakanishi, A. Okiji, J. Appl. Phys. 92 (2002) 5704.
[25] H. Brune, Surf. Sci. Rep. 31 (1998) 121.
[26] M. Michely, J. Krug, Islands, Mounds and Atoms, Springer, Berlin, 2003.
[27] R. Kunkel, B. Poelsema, L.K. Verheij, G. Comsa, Phys. Rev. Lett. 65 (1990) 733.
[28] M. Parschau, K. Christmann, Surf. Sci. 423 (1999) 303.
[29] J.T. Kohlhepp, G.J. Strijkers, H. Wieldraaijer, W.J.M. de Jonge, Phys. Stat. Sol. (a) 189 (2002) 701.